Regular Articles

Experimental Evaluation of High-capacity Wireless Transmission Using Orbital Angular Momentum Multiplexing Technology

Doohwan Lee, Yasunori Yagi, Hirofumi Sasaki, and Hiroyuki Shiba

Abstract

We are researching and developing technology to achieve terabit-class wireless transmission toward six-generation wireless systems. In this article, we present experimental evaluations of high-capacity wireless transmission using orbital angular momentum (OAM) multiplexing on a 40-GHz frequency band with a bandwidth of 1.5 GHz at distances of 100 and 200 m. Our OAM antennas have two uniform circular arrays (UCAs) with the same diameter using different linear polarizations and Butler matrices, which are analog devices for generating and separating OAM modes. OAM beams are generated using a Butler matrix, which is an analog radio-frequency circuit, and radiated from the UCAs. We implemented an OAM multiplexing transmitter (Tx) and receiver (Rx) on the 40-GHz band. The Tx and Rx can generate and separate seven OAM modes (0, ±1, ±2, ±3) and two polarizations (vertical and horizontal), which is a total of 15 streams including the center antenna element to transmit OAM mode 0. Each channel carries a 1.5-Gbaud signal. We experimentally evaluated the transmission capacity at distances of 100 and 200 m. The results indicate successful wireless data transmission of 137 Gbit/s at a distance of 100 m and 117 Gbit/s at a distance of 200 m.

Keywords: orbital angular momentum (OAM), point-to-point, line-of-sight, uniform circular array, 40-GHz band

1. Introduction

The demand for achieving high-capacity wireless transmission is increasing due to exponentially increasing data traffic toward six-generation (6G) wireless systems [1]. The use of wireless transmission is expected to increase in all fields including connected cars, virtual reality/augmented reality, three-dimensional cameras, and high-definition video transmission. Considering such an increase, it is anticipated that the hundreds-of-gigabit level to terabit level wireless transmission will be necessary in the 2030s [2–4].

There have been many reports on high-capacity wireless transmission in orbital angular momentum (OAM) and multiple-input multiple-output (MIMO)/single-input single-output (SISO) multiplexing [5–17], as shown in **Fig. 1**. We provide a summary of these reports below. There have been reports on experiments over 100 Gbit/s in short distances (<10 m) in laboratory environments, and approximately 100 Gbit/s in outdoor environments (≥100 m). In terms of transmission capacity, 1.056-Tbit/s wireless transmission over 3.6 m was reported by GTEC, Fudan University using 4×4 MIMO on D-band [5]. In terms of transmission distance, Northrop Grumman,
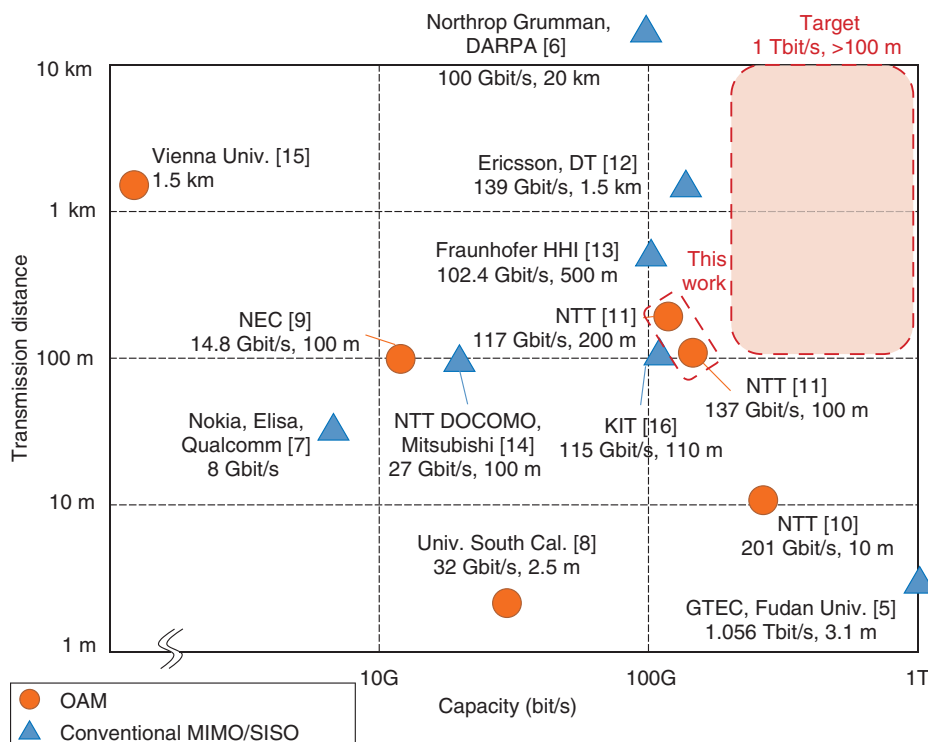
Fig. 1. Reports of experimental demonstration on high-capacity wireless transmission using conventional MIMO/SISO and wireless OAM transmission.

DARPA [6] reported 100-Gbit/s wireless transmission (total rate of transmission and reception) at a distance of 20 km. The result from 5G commercial networks was the 8-Gbit/s transmissions reported by Nokia, Qualcomm, and Elisa [7]. Regarding OAM multiplexing, 32-Gbit/s transmission on the 60-GHz band over 2.5-m distance was reported by University of Southern California [8], and 14.8-Gbit/s transmission on the 150-GHz band over 100 m using real-time signal processing was reported by NEC [9]. Considering beyond 5G and 6G wireless communication, we set our target to 1 Tbit/s and over 100-m transmission.

To achieve such terabit-class wireless transmission, we are researching OAM multiplexing transmission technology as a new spatial multiplexing technology that enables high-capacity wireless transmission. We previously reported on experiments of over 200-Gbit/s transmission using OAM-MIMO multiplexing on the 28-GHz band at a distance of 10 m in a shielded room [10]. We further achieved wireless data transmission of 137 Gbit/s at a distance of 100 m and 117 Gbit/s at a distance of 200 m [11] using OAM multiplexing on the 40-GHz band. The remainder of this article reports on the principle of OAM multiplexing and our

recent research.

2. OAM multiplexing technology

2.1 Principle

OAM is a physical property of electro-magnetic waves characterized by a helical phase front in the propagation direction. Since these characteristics can be used to create multiple orthogonal channels, wireless communication using OAM can increase radio-spectrum efficiency and expand the capacity of the scarce radio spectrum. The number of phase rotations is called an OAM mode. Different data signals can be transmitted at the same time by transmitting different signals using radio waves having different OAM modes [8].

Given an electromagnetic wave having this OAM property, the trace of the same phase takes on a helical shape in the direction of propagation (**Fig. 2**). For example, Figure 2(a) illustrates the trance of the same phase in OAM modes 1, 2, and 3. Radio waves having this OAM property cannot be received without a receiver (Rx) having the same number of phase rotations at the time of transmission. For this reason, if
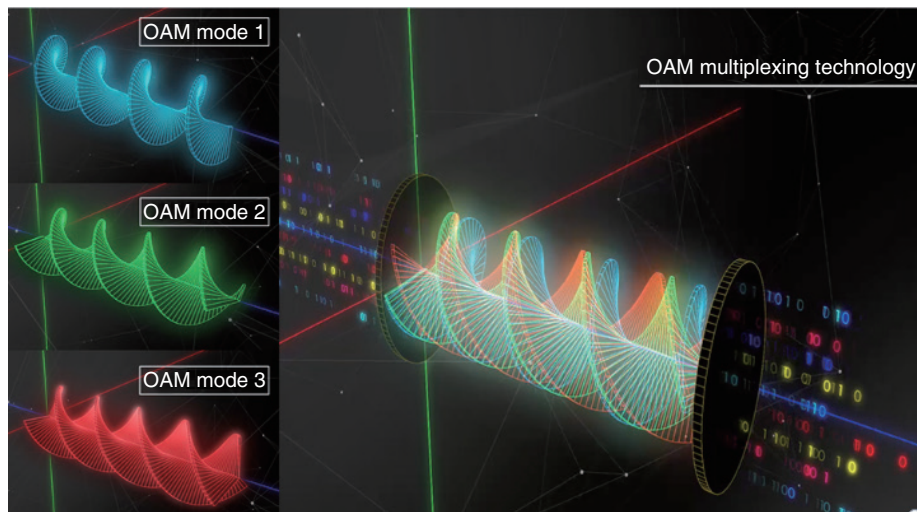
(a) Trace of the same phase   (b) Concurrent transmission

Fig. 2.   Principle of OAM multiplexing transmission technology.

multiple radio waves having different OAM modes are superposed, they can eventually be separated without mutual interference as long as an Rx is prepared that can receive radio beams with the same phase rotations corresponding to each OAM mode. Figure 2(b) shows an example in which different signals are put on OAM modes 1, 2, and 3 and transmitted simultaneously. Technology for transmitting multiple data signals using this feature is called OAM multiplexing transmission technology.

2.2   Generation and separation
To generate a beam carrying the OAM mode n (L = n), antenna elements are connected with phase shifters that make n × 360 degrees of rotations. **Figure 3(a)** shows an example of beam generations of OAM modes 0, 1, and 2 using a uniform circular array (UCA) consisting of 8 antenna elements. Note that concurrent transmission of multiple OAM modes can be achieved by superposing multiple OAM signals, as in **Fig. 3(c)**.

The separation of beams carrying OAM modes can be done in a similar manner as generation using antenna elements connected with phase shifters that make opposite direction of rotations. As far as the number of antenna elements are larger than 2n, n × 360 degrees of rotations are orthogonal one another. Therefore, the separation of each OAM mode from a mixed OAM mode signal can be done without aliasing. **Figure 3(b)** shows an example of the phase of

each antenna element corresponding to the example above.

2.3   Transmission and reception
The beams with different OAM modes can be approximately generated or separated simultaneously using a UCA with a discrete Fourier transform (DFT). They are orthogonal as long as they propagate coaxially. Mathematically, the channel between UCAs is a circulant matrix, so the channel can be diagonalized using a DFT matrix as the singular value decomposition (SVD) method, meaning oppositely arranged transmitting and receiving UCAs can create several isolated channels regardless of the propagation distance. Theoretically, the OAM has an infinite depth of field, but the discretization of space sampling limits the maximum number of available OAM modes when using a UCA and DFT processor. The maximum number is equal to the number of antenna elements in a UCA. When using UCAs for transmitting and receiving antennas, the beam propagation with OAM modes can be analyzed using the standard narrow band MIMO theory.

We now discuss the theoretical background of an OAM multiplexing system with UCAs. **Figure 4** shows a schematic chart of OAM multiplexing transmission. When UCAs are placed opposite each other, the antenna-array configuration is axisymmetric so that the channel matrix becomes circulant. When the number of antenna elements in a UCA is defined as n,
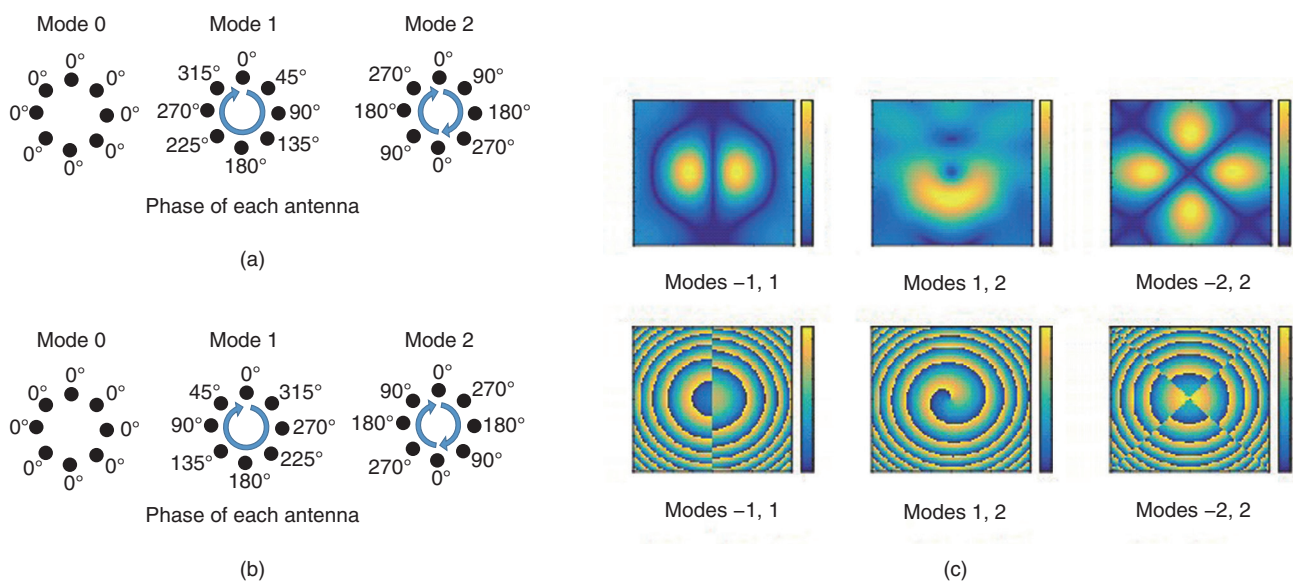
Fig. 3. (a) Generation of OAM modes with a UCA, (b) separation of OAM modes with a UCA, (c) intensity distribution (above) and phase distribution (below) of combined OAM modes (L is the number of OAM modes).
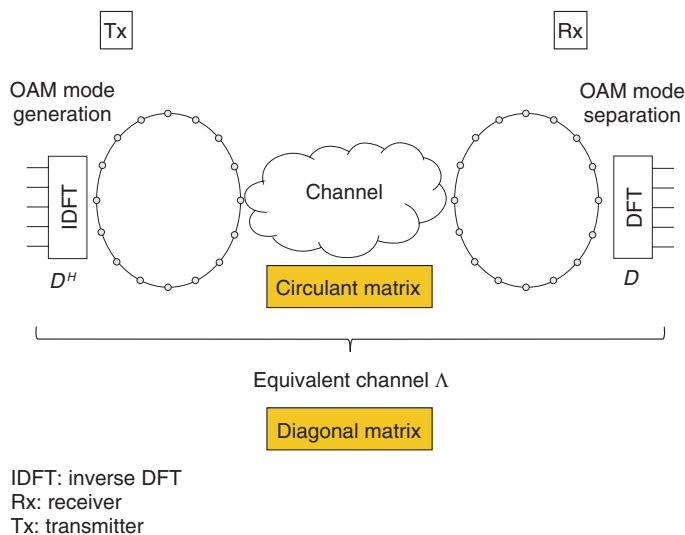

IDFT: inverse DFT
Rx: receiver
Tx: transmitter

Fig. 4. Schematic of OAM multiplexing system.

the circulant matrix is diagonalized using the $n \times n$ DFT matrix

$$D_n (x, y) = \exp\left(-j\left(\frac{2\pi(x - 1)}{n}\right) l(y)\right) /\sqrt{n},$$ (1)

as

$$H = D_n \Sigma D_n{}^H,$$ (2)

$$\Lambda = \Sigma = \begin{pmatrix} \lambda_{l(1)} & & & 0 \\ & \lambda_{l(2)} & & \\ & & \ddots & \\ 0 & & & \lambda_{l(n)} \end{pmatrix},$$ (3)

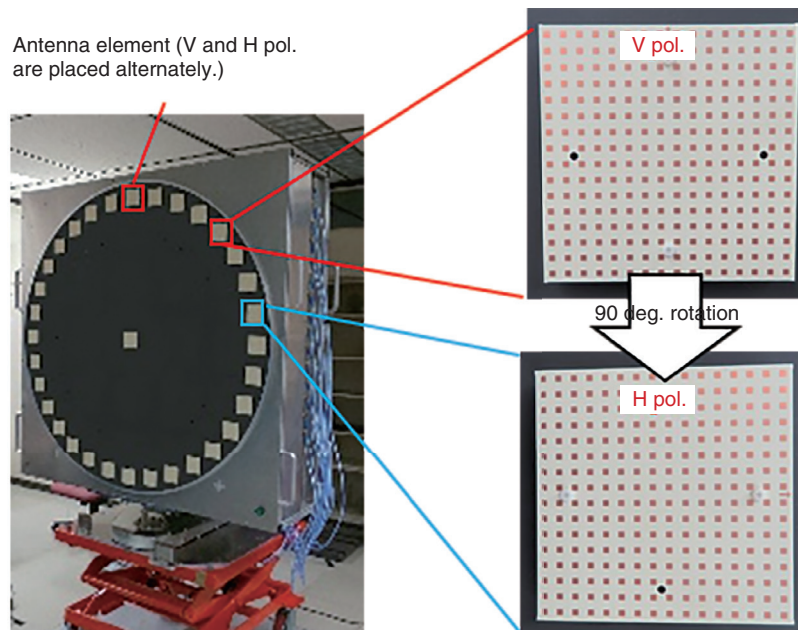where l denotes OAM mode corresponding to the yth

Fig. 5. Prototype of OAM transmission equipment.

eigenvector, H and Σ denote the channel matrix between the receiving and transmitting UCAs and diagonal matrix, respectively, and Λ denotes the equivalent channel matrix including DFT processing, as shown in Fig. 4.

One of the strengths of OAM multiplexing is that it only requires static processing and DFT, so we can use analog devices for OAM-mode generation and separation without digital signal processing. A Butler matrix is an analog circuit that can process DFT calculations with hybrid circuits and phase shifters, so we used it for OAM-mode generation and separation in our system [11, 17].

3. Transceiver design

We designed a 40-GHz-band OAM multiplexing transceiver to conduct outdoor experiments. **Figure 5** shows this transceiver and its antenna elements. The diameter of the UCA is 120 cm, and a total of 33 antenna elements (16 elements each for vertical (V) and horizontal (H) polarization UCA and the center) are placed on the circumference. The antenna size depends on the frequency, as shown in **Table 1**. The size can be reduced when higher frequency bands are used. The gain of the antenna element is 25 dBi. This antenna element can radiate V or H polarization by rotating 90 degrees. One antenna element is placed on

Table 1. Equivalent antenna sizes.

Frequency band [GHz]	40	90	150	300
Antenna size [mm]	1200	800	620	440

the center of a UCA to transmit mode 0 at the singular points of the OAM mode.

Figure 6 shows a block diagram of the OAM-transmission experiment. Baseband (BB) signal waveforms generated by Matrix Laboratory were input to the transmitter (Tx) using arbitrary waveform generators (AWGs). Analog BB signals were up-converted to radio frequencies (RFs) of 39.5 to 41 GHz signals in the Tx. Finally, 7 OAM modes signals were generated and multiplexed using Butler matrices in each polarization and transmitted from the 16 antenna elements. The mode isolation of these Butler matrices was over 15 dB [17]. We designed 7×16 Butler matrix working on the 40-GHz band for DFT processing to generate and separate seven OAM modes (OAM modes 0, ±1, ±2, ±3). We first designed 8×16 Butler matrices and terminated a port for OAM mode 4. By using these Butler matrices, we can reduce RF chains because we just prepare the RF chains for the OAM modes used to multiplex rather than for all antenna elements.

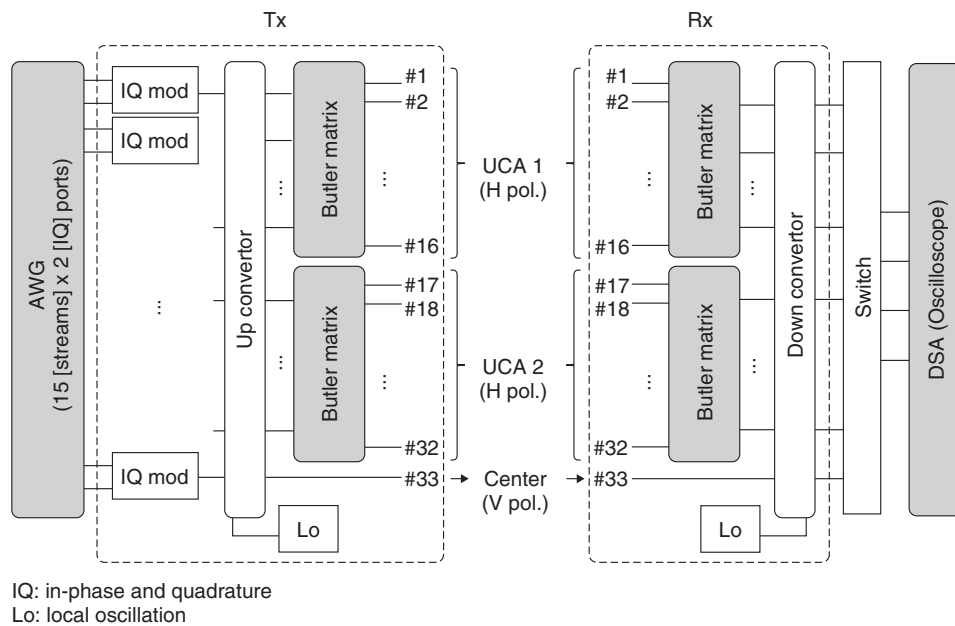The OAM beams were propagated to the Rx. The

IQ: in-phase and quadrature
Lo: local oscillation

Fig. 6. Block diagram of our experiment.

Table 2. System specifications.

Parameters	Values	Parameters	Values
OAM modes	−3, −2, −1, 0, 1, 2, 3	Baud rate	1.5 Gbaud
Polarization	V/H	FFT size/CP size	1024/16 symbols
Diameter of UCA	120 cm	FEC (outer/inner)	BCH/LDPC
Num. of antennas	16 elements/pol. & center	Equalization	SC-FDE/MMSE
Antenna gain	25 dBi/element	Modulation (prepared)	QPSK–1024QAM
Frequency	39.5–41 GHz	Coding rate (prepared)	1/2, 3/5, 2/3, 3/4, 4/5, 5/6, 8/9, 9/10

CP: cyclic prefix
FFT: fast Fourier transform
MMSE: minimum mean square error
QAM: quadrature amplitude modulation

QPSK: quadrature phase-shift keying
SC-FDE: single-carrier frequency domain
    equalization

Rx was embedded with a variable attenuator, which made it possible to adjust the received signal level appropriately even if the received power varies with the transmission distance. The received signals were separated for each OAM mode signal by using the Butler matrices and down-converted to intermediate frequency (IF) signals. Finally, the digital serial analyzer (DSA) stored and saved the IF signals as waveform data. The saved waveforms were demodulated by MATLAB off-line signal processing, and we evaluated the transmission capacity. We coded the multiplexed data streams with a low-density parity-check (LDPC) code and Bose-Chaudhuri-Hocquenghem (BCH) code with a frame length of 64,800 bits on the basis of the Digital Video Broadcasting - Satellite - Second Generation (DVB-S2) standard used as forward error collection (FEC). We applied an adaptive modulation and coding algorithm with which the modulation order and adaptively determined the coding rate depending on the signal-to-noise ratios (SNRs). We prepared error-free SNR ranges in advance as a table for each modulation order and coding rate. We summarize the system specifications of the OAM transmission in **Table 2**.
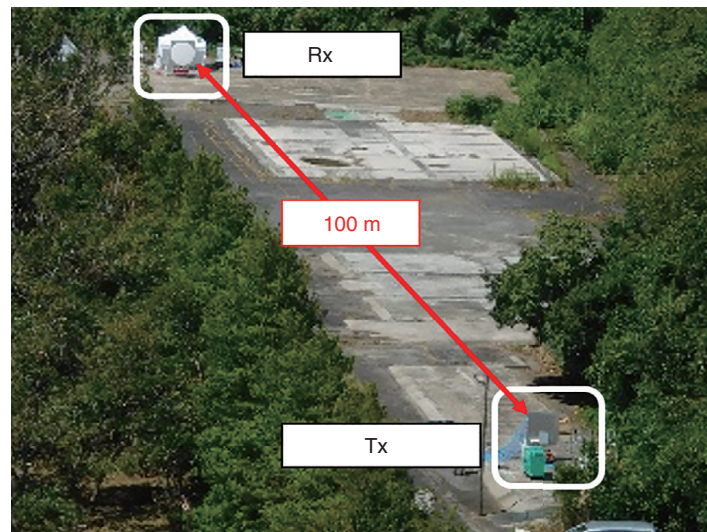
Fig. 7.   Experimental environment for wireless OAM multiplexing transmission at a distance of 100 m in the field.

4.   Experimental evaluations

4.1   Experimental setup

Table 2 lists the specific parameters of our experimental setup. We multiplexed 15 data streams using 7 OAM modes and 2 UCAs with different linear polarizations in both transmitting and receiving antennas. We then designed antenna elements in the UCAs, which were patch antenna arrays with an antenna gain of 25 dBi, as shown in Fig. 5. The isolation between different linear polarizations of the antenna elements was more than 30 dB on average across the whole bandwidth. In accordance with the relationship between effective bits in a symbol and SNR of our digital signal processing and the symbol rate of 1.5 GHz, roughly a 20-dB SNR on average of 15 data streams is enough to obtain more than 100 Gbit/s. The amount of transmitting power and antenna gains was roughly 53 dB. The channel gain was then roughly –90 dB, and the noise floor including the receiver noise figure was –67.7 dBm. We thus determined that our experimental system was able to obtain more than a 20-dB SNR on average across all of OAM modes.

4.2   Experimental results

We conducted outdoor wireless transmission experiments at distances of 100 and 200 m. Each distance was a line-of-sight environment, as shown in **Figs. 7** and **8**, respectively. The alignment between the Tx and Rx was conducted using a laser rangefinder placed at the corner of the antenna. Error-free trans-
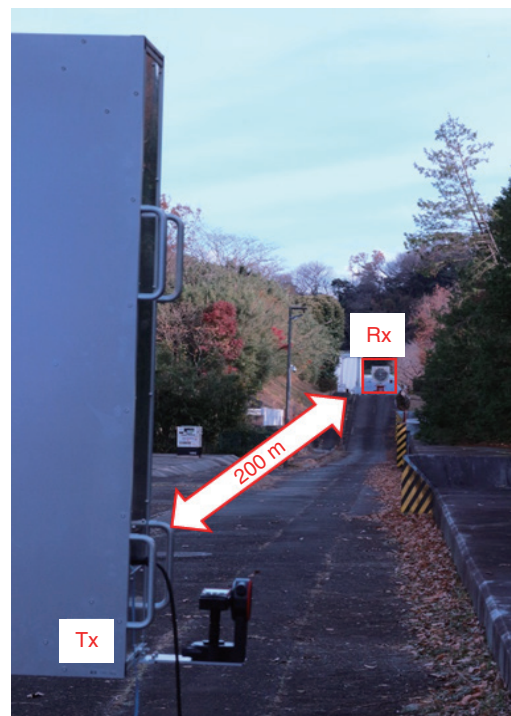

Fig. 8.   Experimental environment for wireless OAM multiplexing transmission at a distance of 200 m in the field.

mission with channel coding was 137.3 Gbit/s with 15 streams at a distance of 100 m. The spectral efficiency was 91.5 bit/s/Hz. The 200-m error-free

64QAM
OAM mode –2 (V pol.)
SNR: 21.03 dB
BER (w/o FEC): 0.428%

256QAM
OAM mode 0 (V pol.)
SNR: 24.55 dB
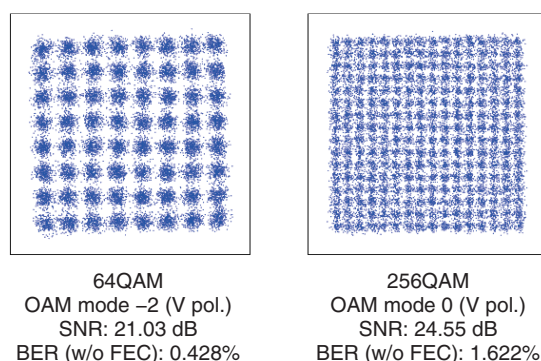BER (w/o FEC): 1.622%

Fig. 9.   Representative constellation diagrams of 64 QAM and 256 QAM.

Table 3.   The receiving SNRs, modulation, and coding rate during transmission experiment at distances of 100 and 200 m.

Order	100-m transmission			200-m transmission		
	Transmission capacity [Gbit/s]	Modulation	Coding rate	Transmission capacity [Gbit/s]	Modulation	Coding rate
#1	11.25	1024QAM	3/4	11.25	1024QAM	3/4
#2	10.80	256QAM	9/10	10.80	256QAM	9/10
#3	10.80	256QAM	9/10	10.80	256QAM	9/10
#4	10.80	256QAM	9/10	10.80	256QAM	9/10
#5	10.80	256QAM	9/10	10.80	256QAM	9/10
#6	10.80	256QAM	9/10	10.80	256QAM	9/10
#7	10.80	256QAM	9/10	10.67	256QAM	8/9
#8	10.67	256QAM	8/9	9.60	256QAM	4/5
#9	10.00	256QAM	5/6	8.10	64QAM	9/10
#10	9.60	256QAM	4/5	7.20	64QAM	4/5
#11	9.60	256QAM	4/5	6.00	64QAM	2/3
#12	8.10	64QAM	9/10	4.80	16QAM	4/5
#13	6.75	64QAM	3/4	3.60	16QAM	2/3
#14	4.00	16QAM	2/3	2.25	QPSK	3/4
#15	2.50	QPSK	5/6			
Total	137.27 Gbit/s			117.47 Gbit/s		

transmission with channel coding was 117.5 Gbit/s with 14 streams. **Figure 9** shows the representative measured constellations of 64 quadrature amplitude modulation (QAM) and 256 QAM. The SNRs were 21.03 and 24.55 dB, and the bit error rates (BERs) without FEC were 0.428 and 1.622%. We transmitted a few data frames and confirmed reproducibility. The spectral efficiency was 78.3 bit/s/Hz. The multiplex number of 14 at 200 m was due to the modified water-filling-power allocation and providing a margin for determining modulation and coding rates. **Table 3** shows the transmission capacity, modulation, and coding rate of each stream. They are listed in descending order of transmission capacity, that is, the order of the receiving SNR. The modulations used were from quadrature phase-shift keying (QPSK) to 1024 QAM for each stream, and transmission rates were up to 11.25 Gbit/s. We previously reported the achievement of 119.7 Gbit/s transmission at a distance of 100 m and showed that similar capacity can be achieved at a distance of 200 m.

5. Discussion and conclusion

We designed transmitting and receiving antennas of OAM multiplexing for over 100-Gbit/s wireless transmission at a distance of 100 m. Our antennas have two UCAs with 16 antenna elements for different linear polarizations, and Butler matrices for OAM-mode generation and separation. Therefore, we could use two orthogonal bases of seven OAM modes (OAM mode 0, ±1, ±2, ±3) and dual polarization. An antenna element of V-pol. was arranged at the center of each antenna. The radio wave transmitted from the center antenna element was OAM mode 0, which provided an additional data stream for multiplexing. Note that there were two data streams in OAM mode 0 of V-pol., which were not orthogonal to each other. However, they had different eigenvectors for the radius direction, so they could be isolated by traditional MIMO-based digital signal processing. We conducted a transmission experiment using OAM multiplexing in the field at distances of 100 and 200 m. We confirmed that the transmission capacity of over 100 Gbit/s can be achieved even at 200 m. We implemented offline signal processing including transmit precoding based on SVD and the OAM multiplexing Tx and Rx on the 40-GHz band. This Tx and Rx can generate and separate seven OAM modes (−3, −2, −1, 0, 1, 2, 3) by using Butler matrices for each polarization. Each channel carries a 1.5-Gbaud signal. The results indicate that wireless data transmissions of 137.3 Gbit/s at a distance of 100 m and 117.5 Gbit/s at a distance of 200 m were successful. The spectral efficiency was respectively 91.5 and 78.3 bit/s/Hz at 100 and 200 m.

References

[1] DOCOMO 6G White Paper, Feb. 2021.
https://www.nttdocomo.co.jp/english/corporate/technology/whitepaper_6g/
[2] The 3rd Generation Partnership Project (3GPP), https://www.3gpp.org/
[3] Y. Corre, G. Gougeon, J. Doré, S. Bicaïs, B. Miscopein, E. Faussurier, M. Saad, J. Palicot, and F. Bader, "Sub-THz Spectrum as Enabler for 6G Wireless Communications up to 1 Tbps," Presented at 6G Wireless Summit, Mar. 2019.
http://www.6gsummit.com/wp-content/uploads/2019/04/Day3_Session7_Corre_SIRADEL.pdf
[4] SAMSUNG's 6G White Paper, Jul. 2020.
[5] X. Li, J. Yu, L. Zhao, K. Wang, C. Wang, M. Zhao, W. Zhou, and J. Xiao, "1-Tb/s Millimeter-wave Signal Wireless Delivery at D-band," J. Lightw. Technol., Vol. 37, No. 1, pp. 196–204, Jan. 2019.
[6] Press release issued by Northrop Grumman, "Northrop Grumman, DARPA Set New Standard for Wireless Transmission Speed," Aug. 2018.
https://news.northropgrumman.com/news/releases/northrop-grumman-darpa-set-new-standard-for-wireless-transmission-speed
[7] Press release issued by Nokia, "Nokia, Elisa and Qualcomm Achieve 5G Speed Record in Finland," Nov. 2020.
https://www.nokia.com/about-us/news/releases/2020/11/18/nokia-elisa-and-qualcomm-achieve-5g-speed-record-in-finland/
[8] Y. Yan, L. Li, Z. Zhao, G. Xie, Z. Wang, Y. Ren, N. Ahmed, S. Sajuyigbe, S. Talwar, M. Tur, N. Ashrafi, S. Ashrafi, A. F. Molisch, and A. E. Willner, "32-Gbit/s 60-GHz Millimeter-wave Wireless Communication Using Orbital Angular Momentum and Polarization Multiplexing," Proc. of IEEE International Conference on Communications (ICC) 2016, May 2016.
[9] Press release issued by NEC, "NEC Successfully Demonstrates Real-time Digital OAM Mode Multiplexing Transmission over 100m in the 150GHz-band for the First Time," Mar. 2020.
https://www.nec.com/en/press/202003/global_20200310_01.html
[10] Y. Yagi, H. Sasaki, T. Yamada, and D. Lee, "200 Gbit/s Wireless Transmission Using Dual-polarized OAM-MIMO Multiplexing on 28 GHz Band," Proc. of IEEE GLOBECOM Workshop on HCPtP, Dec. 2019.
[11] Y. Yagi, H. Sasaki, T. Semoto, T. Kageyama, T. Yamada, J. Mashino, and D. Lee, "Field Experiment of 117 Gbit/s Wireless Transmission Using OAM Multiplexing at a Distance of 200 m on a 40 GHz Band," Proc. of IEEE ICC Workshop on OAMT, June 2021.
[12] C. B. Czegledi, M. Hörberg, M. Sjödin, P. Ligander, J. Hansryd, J. Sandberg, J. Gustavsson, D. Sjöberg, D. Polydorou, and D. Siomos, "Demonstrating 139 Gbps and 55.6 bps/Hz Spectrum Efficiency Using 8×8 MIMO over a 1.5-km Link at 73.5 GHz," Proc. of 2020 IEEE/MTT-S International Microwave Symposium (IMS), Aug. 2020.
[13] C. Castro, R. Elschner, T. Merkle, C. Schubert, and R. Freund, "Experimental Demonstrations of High-capacity THz-wireless Transmission System for Beyond 5G," IEEE Commun. Mag, Vol. 58, No. 11, pp. 41–47, Nov. 2020.
[14] Press release issued by NTT DOCOMO, "Mitsubishi Electric and NTT DOCOMO Achieve World's First 27Gbps Throughput in 5G Outdoor Trials," Nov. 2018.
https://www.nttdocomo.co.jp/english/info/media_center/pr/2018/1122_00.html
[15] M. Krenn, R. Fickler, M. Fink, J. Handsteiner, M. Malik, T. Scheidl, R. Ursin, and A. Zeilinger, "Communication with Spatially Modulated Light through Turbulent Air across Vienna," New J. Phys., Vol. 16, No. 11, Nov. 2014.
[16] T. Harter, C. Füllner, J. N. Kemal, S. Ummethala, J. L. Steinmann, M. Brosi, J. L. Hesler, E. Bründermann, A.-S. Müller, W. Freude, S. Randel, and C. Koos, "Generalized Kramers-Kronig Receiver for Coherent Terahertz Communications," Nat. Photonics, Vol. 14, pp. 601–606, Sept. 2020.
[17] H. Sasaki, Y. Yagi, T. Yamada, T. Semoto, and D. Lee, "An Experimental Demonstration of over 100 Gbit/s OAM Multiplexing Transmission at a Distance of 100 m on 40 GHz Band," Proc. of IEEE ICC Workshop on OAMT, June 2020.

Doohwan Lee

Distinguished Researcher, Wave Propagation Laboratory, NTT Network Innovation Laboratories.

He received a B.S. (Hons.) and M.S. in electrical engineering from Seoul National University, South Korea, in 2004 and 2006, and Ph.D. in electrical engineering and information systems from the University of Tokyo in 2009. He has been with NTT Network Innovation Laboratories since 2009. From 2012 to 2014, he was an assistant professor at the Research Center for Advanced Science and Technology, the University of Tokyo. Since 2016, he has been a part-time lecturer at Kanagawa University. His research interests include compressed sensing, software/cognitive radio, signal processing, and OAM multiplexing. He received the Best Paper Award and Best Technical Exhibition Award from the Institute of Electronics, Information and Communication Engineers (IEICE) Software Radio in 2011, the IEICE Communications Society Excellent Paper Award in 2012, the IEICE SRW (Short Range Wireless Communications) Young Researcher's Award in 2016, the Best Technical Exhibition Award from SmartCom 2014, the Best Paper Award from SmartCom 2016, the Best Paper Award and Special Technical Award in Smart Radio from IEICE Smart Radio in 2017, and the Distinguished Contributions Award from IEICE Communications Society in 2021.
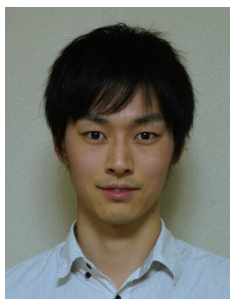
Yasunori Yagi

Researcher, Wave Propagation Laboratory, NTT Network Innovation Laboratories.

He received a B.E. and M.E. in electrical engineering from Tokyo University of Science in 2015 and 2017. He joined NTT Network Innovation Laboratories in 2017 and has been engaged in research on high-capacity wireless system.

Hirofumi Sasaki

Researcher, Wave Propagation Laboratory, NTT Network Innovation Laboratories.

He received a B.E. and M.E. in engineering from Osaka University in 2011 and 2013. He joined NTT Network Innovation Laboratories in 2013, where he was engaged in research on heterogeneous wireless network system in spectrum sharing scenarios. Since 2015, he has been engaged in research on super high-speed wireless communication in millimeter-wave regions. He received the Best Paper Award from the IEICE SmartCom 2016, the Best Paper Award and Special Technical Award in Smart Radio from the IEICE Smart Radio in 2017, Young Researcher Award from IEICE in 2017. He served as the secretary of IEEE GLOBECOM 2019 Workshop on High Capacity Point-to-Point Wireless Communications (HCPtP 2019) and GLOBECOM 2020 Workshop on High Capacity Wireless Communications (HCWC 2020).

Hiroyuki Shiba

Senior Research Engineer, Supervisor, Wave Propagation Laboratory, NTT Network Innovation Laboratories.

He received a B.E. and M.E. from Gunma University in 1995 and 1997 and Ph.D. from Waseda University, Tokyo, in 2014. Since joining NTT Wireless Systems Laboratories in 1997, he has been engaged in research on software-defined radio, cognitive radio technologies, and flexible wireless systems. He is currently engaged in research and development of high-capacity wireless systems. He is a senior member of IEICE.